

Self-calibration of weak lensing cosmic shear biases

G. Congedo,^{1*} A. N. Taylor,¹

¹*Institute for Astronomy, University of Edinburgh, Royal Observatory, Blackford Hill, Edinburgh EH9 3HJ, UK*

Accepted XXX. Received YYY; in original form ZZZ

ABSTRACT

In order to reach the required performance of Stage-III and IV weak lensing surveys, cosmic shear measurements have to rely on external simulations to calibrate residual biases. Over the years, several techniques have been developed to mitigate the impact of residual biases prior to calibration, including the inference of shear responses on images to correct multiplicative biases, and the empirical correction of additive biases. We introduce a novel methodology that generalises upon the state-of-the-art approaches by inferring multiplicative and additive biases jointly from parameterised distributions of measured ellipticities, crucially without relying on external simulations and independently from cosmology. Shear biases are marginalised over the unknown hyperparameters in the modelling, hence mitigating the impact of degeneracies. We apply the technique to a representative problem and show the performance of the estimation, even in the presence of noise. The method has a high potential for applicability to the calibration of weak lensing cosmic shear in current and future lensing surveys.

Key words: cosmology: observations – gravitational lensing: weak – methods: statistical

1 INTRODUCTION

With the advent of Stage-IV galaxy surveys represented by the three main wide-field telescopes [*Euclid*, [Euclid Collaboration: Mellier et al. \(2025\)](#); *Rubin*, [Ivezić et al. \(2019\)](#); and *Roman*, [Spergel et al. \(2015\)](#)], cosmological measurements will soon enter the regime of percent-level precision. One of the main cosmological probes is weak lensing cosmic shear, the distortion of images of background galaxies due to the large-scale structure in the foreground ([Schneider 2005](#); [Kilbinger 2015](#)). Although weak lensing is a promising technique for constraining the cosmological parameters of dark matter, dark energy and modified gravity, Stage-III surveys have had to correct systematic errors with simulations in order to reach the desired accuracy of cosmological measurements ([Fenech Conti et al. 2017](#); [Mandelbaum et al. 2018](#); [Kannawadi et al. 2019](#); [MacCrann et al. 2022](#); [Li et al. 2022, 2023a,b](#)).

One of the key sources of systematic errors is the modelling of the telescope’s point-spread function (PSF), since residual errors propagate through the inferred cosmic shear. In fact, PSF ellipticity errors induce additive biases in galaxy measurements, whereas PSF size errors induce multiplicative biases ([Paulin-Henriksson et al. 2008](#)). Moreover, detector effects also introduce additional additive biases, such as for the case of charge transfer inefficiency ([Rhodes et al. 2010](#)), but sometimes also multiplicative errors, such as for the case of the bright-fatter effect ([Antilogus et al. 2014](#)). Even in the idealistic situation where the PSF might be perfectly known, there are always multiplicative biases introduced by the measurement methodology (see, e.g., [Miller et al. 2013](#); [Euclid Collaboration: Congedo et al. 2024](#)) or due to the non-uniform distribution of galaxies (see, e.g.,

[Euclid Collaboration: Martinet et al. 2019](#); [MacCrann et al. 2022](#); [Euclid Collaboration: Congedo et al. 2024](#)).

Over the years, much effort has been put initially towards understanding the source of fundamental biases due to the measurement process ([Melchior & Viola 2012](#); [Refregier et al. 2012](#); [Hall & Taylor 2017](#)) and later towards trying to correct measurement and selection biases directly in the measurement process itself ([Bernstein & Armstrong 2014](#); [Sheldon 2014](#); [Bernstein et al. 2016](#); [Huff & Mandelbaum 2017](#); [Sheldon & Huff 2017](#); [Sheldon et al. 2020](#); [Hoekstra et al. 2021](#); [Hoekstra 2021](#)). However, with much stringent lensing accuracy required for a Stage-IV survey like *Euclid* ([Massey et al. 2013](#); [Cropper et al. 2013](#)), residual biases still have to be corrected for via simulations, which raise questions about the sensitivity of the calibration on the simulation setup or the data volume required for the correction ([Hoekstra et al. 2017](#); [Pujol et al. 2019](#); [Jansen et al. 2024](#); [Euclid Collaboration: Congedo et al. 2024](#)).

Residual additive shear biases are known to be more forgiving in that they can be empirically corrected directly on the data, which allow us to capture their spatial dependence (see, e.g., [van Uitert & Schneider 2016](#); [Hildebrandt et al. 2020](#); [Kitching et al. 2021](#)). In fact, this methodology is general enough to be easily applied to any broad sample, including tomographic, angular, or morphological bins. However, multiplicative biases are notoriously much harder to correct and recent developments have focussed primarily on estimating the sensitivity of the shear measurements and selections to an input shear, with a procedure called METACALIBRATION/METADETECTION yielding shear responses as direct proxies for multiplicative biases ([Huff & Mandelbaum 2017](#); [Sheldon & Huff 2017](#); [Sheldon et al. 2020, 2023](#)). However, there is sensible expectation that even those methodologies may not be fully immune to residual biases, especially when applied to Stage-IV surveys where the requirements and precision are much more stringent than Stage

* E-mail: giuseppe.congedo@ed.ac.uk

III, and therefore simulations are still required to correct for residual biases.

In this paper, we propose a novel method to estimate residual additive and multiplicative biases in a unified, general approach. Our methodology infers multiplicative and additive biases directly from the data and without relying on assumptions about morphologies or cosmology. Our paper is structured as follows: Sec. 2 presents the general properties of the transformation of ellipticity distributions under the effect of biases; Sec. 3 introduces the Bayesian inference of multiplicative and additive biases from empirical distributions of ellipticity while marginalising over nuisance parameters; Sec. 4 tests the procedure on representative data and shows the performance of our estimator, also discussing potential limitations; Sec. 5 draws the main conclusions.

2 BIASED ELLIPTICITY DISTRIBUTIONS

We wish to understand the properties of the transformation between the distribution of true galaxy ellipticities and that of measured galaxy ellipticities under the effect of shear biases. We assume that the biases are constant and defined as effective quantities for a broad sample selection. In this context, the true galaxy ellipticity, ϵ , is a spin-2 complex number representing the lensed ellipticity of a galaxy before the measurement (Seitz & Schneider 1997),

$$\epsilon = \frac{\epsilon_s + g}{1 + \epsilon_s g^*}, \quad (1)$$

where ϵ_s is the intrinsic ellipticity of the source galaxy, g is the reduced shear, $g = \langle \epsilon \rangle$, and $\epsilon \approx \epsilon_s + g$ in the weak-lensing regime (Schneider 2005; Kilbinger 2015). After the measurement, the measured galaxy ellipticity, $\hat{\epsilon}$, will include statistical noise and bias.¹ With both ϵ_s and g being zero-mean random variables, ϵ follows a symmetric distribution centred at zero with $|\epsilon| < 1$, except in the case of intrinsic alignments (Joachimi et al. 2015), which should have negligible effect on the mean of a broad sample like a tomographic bin.

Kitching et al. (2021); Euclid Collaboration: Congedo et al. (2024) introduced the most general bias transformation linking measured shear, \hat{g} , and true shear, g , given in terms of a spin-0 or 4 multiplicative biases, m , and a spin-2 additive bias, c . For simplicity, in this paper, we assume a simpler 1D linear model with scalar biases (Guzik & Bernstein 2005; Huterer et al. 2006; Heymans et al. 2006),

$$\hat{g} = (1 + m)g + c + g_n, \quad (2)$$

where m and c are real scalars defined over a large sample of galaxies, including measurement and selection effects, and g_n is zero-mean statistical noise. Because the ellipticity is a point estimator for shear and $\hat{g} = \langle \hat{\epsilon} \rangle$ and $g = \langle \epsilon \rangle$ for large numbers of galaxies, an approximate model of how the ellipticities transform under an ‘effective’ shear bias defined for the entire sample can be derived as follows,

$$\hat{\epsilon} = (1 + m)\epsilon + c + \epsilon_n, \quad (3)$$

where m and c are effective constants and ϵ_n is zero-mean statistical noise. However, the actual relation between measured and true ellipticity will not, in general, be applicable to individual galaxies due to the non-linear response for large ellipticities where the samples may

¹ We will use the adjectives ‘measured’ and ‘observed’ quite interchangeably throughout the paper, meaning that quantities are the result of a noisy, biased measurement process.

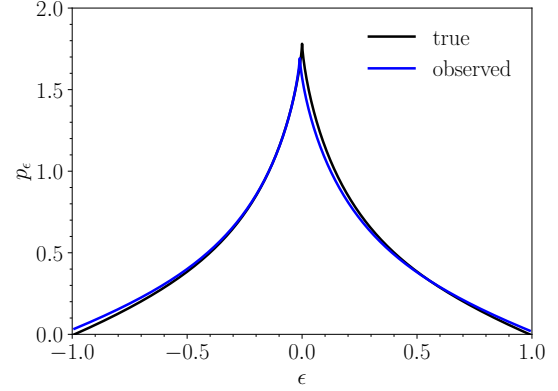


Figure 1. Distribution of true ellipticity and observed ellipticity after the effect of shear biases $m = 0.05$ and $c = -0.01$.

potentially scatter beyond the physical boundaries, or due to the dependence on individual morphologies. We will see that edge effects, which are expected to induce non-linear effects, are down-weighted by our analysis.

According to Eq. (3), the observed 1D-probability distribution of $\hat{\epsilon}$, $p_{\hat{\epsilon}}(\hat{\epsilon})$, is related to the true distribution, $p_{\epsilon}(\epsilon)$, via the conservation of total probability,

$$p_{\hat{\epsilon}}(\hat{\epsilon}|m, c) = \frac{1}{|1 + m|} p_{\epsilon} \left(\frac{\hat{\epsilon} - c}{1 + m} \right) * p_{\epsilon_n}(\epsilon_n), \quad (4)$$

where $p_{\epsilon_n}(\epsilon_n)$ is the distribution of ellipticity noise. For example, Figure 1 shows the impact of $m = 0.05$ and $c = -0.01$ on the shape of the observed distribution. In general, c shifts the mean of the distribution and m rescales the distribution by expansion or contraction, depending on its sign. Additionally, the noise broadens the distribution via a convolutive term. However, the convolution with a random process and the affine/linear operation of biases are fundamentally different in their nature: the former is not reversible while the latter is fully deterministic and, therefore, reversible. Hence, accurate modelling could allow breaking the degeneracy and distinguishing between the two. It is worth noting that the observed distribution in Eq. (4), while seemingly exact, is still an approximation near the physical boundaries because large ellipticities may scatter off simply due to the bias or noise. In fact, real distributions do not show this behaviour and the non-linearity at large ellipticity is naturally built in the observed distribution. Luckily, the effect is small and is down-weighted by our analysis.

The ellipticity distribution is highly non-Gaussian. Empirical distributions show a sharp, cusp-like peak at zero and negative excess kurtosis. This suggests that information on m and c can potentially be extracted at all higher-order moments. It is worth studying what happens to the moments, both central and raw, under the effect of an affine transformation, at least in the limit of negligible noise. The generalisation with random noise proceeds in a similar way, but the equations will be more complicated, showing potential correlations between biases and the noise moments. However, we will see that the noise term can be controlled. The k -th central moment of the measured distribution is

$$\mu_k^0[p_{\hat{\epsilon}}] = (1 + m)^k \mu_k^0[p_{\epsilon}], \quad (5)$$

where the k -th central moment of the true distribution is defined by

$$\mu_k^0[p_{\epsilon}] = \langle (\epsilon - \langle \epsilon \rangle)^k \rangle. \quad (6)$$

As is clear, central moments, by definition, are insensitive to c , but

depend on powers of $1 + m$. For example, measuring the variance ($k = 2$) could, in principle, be sufficient to estimate m if accurate knowledge of the true distribution were available, for example, from deeper observations. Instead, skewness and excess kurtosis,

$$\gamma_1 = \frac{\mu_3^0}{(\mu_2^0)^{3/2}}, \quad (7)$$

$$\gamma_2 = \frac{\mu_4^0}{(\mu_2^0)^2} - 3, \quad (8)$$

are insensitive to m because the same $1 + m$ cancels out at the numerator and denominator in their definitions. Instead, the raw moments of the measured distribution are

$$\mu_k[p_\epsilon] = \sum_{j=0}^k \binom{k}{j} (1+m)^j c^{k-j} \mu_j[p_\epsilon], \quad (9)$$

where the k -th raw moment of the true distribution is defined by

$$\mu_k[p_\epsilon] = \langle \epsilon^k \rangle. \quad (10)$$

Unlike central moments, raw moments are sensitive to a combination of m , c , and noise. In the case of a centred Gaussian distribution, all odd moments are zero and all cumulants beyond the mean and standard deviation are also zero. Therefore, a Gaussian distribution is fully described in terms of its mean and standard deviation and contains very limited information on m and c compared to a more realistic distribution.

The k -th raw moments are also defined in terms of the k -th Taylor coefficients of the moment-generating function. Therefore, it makes sense to derive the relation between moment-generating functions,

$$M_{\hat{\epsilon}}(t) = e^{t \cdot c} \langle e^{t \cdot \epsilon_n} \rangle M_\epsilon^{1+m}(t), \quad (11)$$

where ϵ_n is assumed to be uncorrelated from ϵ and the moment generating function is defined as follows

$$M_\epsilon(t) = \langle e^{t \cdot \epsilon} \rangle, \quad (12)$$

which is also equivalent to the double-sided Laplace transform of p_ϵ . As is clear from Eq. (11), the moment-generating function reduces to the intrinsic function in the limit of negligible noise and biases. In the Fourier domain, the combined effect of c and noise is to add a modulation, while m changes the compactness of the distribution. The Taylor expansion of Eq. (11) yields the moments of the observed distribution and their dependence on m , c , and noise to any order, which we aim to exploit.

3 INFERRING BIASES FROM DATA

We now know that the m -bias is potentially degenerate with the dispersion of the true distribution. If the true dispersion was accurately known, then the degeneracy between m -bias and dispersion would be broken. This observation suggests an effective approach to the problem of inferring biases from the data. Ellipticities, whether true or measured, are always bound to $|\epsilon| < 1$ as not to invalidate the property of an ϵ -ellipticity and its transformation under shear.² Also, observed distributions will be symmetric, although around a non-zero mean, because skewness is invariant under the bias transformation.

² The ϵ -ellipticity of a galaxy is defined as $\epsilon = (a - b)/(a + b) \exp 2i\phi$, where a , b , and ϕ are semi-major axis, semi-minor axis, and rotation angle of the galaxy. This definition, under the shear transformation of Eq. (1), preserves the support of the distribution with $|\epsilon| < 1$.

Additionally, the response of the observed distribution on biases will generally be different in regions around zero or large ellipticities, but it is the cumulative impact on the distribution that matters for shear calibration. All these statistical properties, and in particular the sensitivity of the distribution on biases to any higher-order moments, help to lift the degeneracy in m .

The problem of estimating shear biases from data can be fully framed in Bayesian terms by forward modelling the effect that biases can have on the distribution as a whole without limiting ourselves to just low-order moments. Let $\hat{p}_{\hat{\epsilon},i}$ be the empirical probability distribution function of the measured ellipticities for a relatively large, representative sample, and $\hat{\epsilon}_i$ the observed ellipticity of the i -th bin.³ This empirical distribution is the data we wish to fit with a model for the true distribution, $p_\epsilon(\epsilon|\theta)$, where θ is the vector of hyper-parameters. We must also include the bias transformation in the modelling, to transform from the true distribution to the observed, biased distribution. The probability of observing the ‘data’ distribution, $\hat{p}_{\hat{\epsilon},i}$, given the ‘model’, $p_\epsilon(\hat{\epsilon}_i|m, c, \theta)$ parameterised according to Eq. (4), is denoted with $\pi(\hat{p}_{\hat{\epsilon}}|m, c, \theta)$ and is a likelihood of the model parameters, m , c , and θ . Since bin counts follow a Poisson distribution, this likelihood is the product of many individual Poisson distributions,

$$\ln \pi(\hat{p}_{\hat{\epsilon}}|m, c, \theta) = N \Delta \sum_i \hat{p}_{\hat{\epsilon},i} \ln p_\epsilon(\hat{\epsilon}_i|m, c, \theta) + \text{const}, \quad (13)$$

where N is the number of samples and Δ is the bin width. The likelihood includes the additional constraint on the model, $\Delta \sum_i p_\epsilon(\hat{\epsilon}_i|m, c, \theta) = 1$ and the term $\ln(N \Delta p_{\hat{\epsilon},i})$, both absorbed by the constant. Thanks to the logarithm, the likelihood naturally down-weights the points with low probability or low counts. According to the central limit theorem, the likelihood converges to a Gaussian very rapidly, but in general the Poisson assumption remains more accurate, particularly for small number of samples.

By the Bayes theorem, the joint posterior distribution of shear biases and distribution hyper-parameters given the empirical distribution is

$$\pi(m, c, \theta|\hat{p}_{\hat{\epsilon}}) = \frac{\pi(\hat{p}_{\hat{\epsilon}}|m, c, \theta) \pi(m, c, \theta)}{\pi(\hat{p}_{\hat{\epsilon}})}, \quad (14)$$

where $\pi(m, c, \theta)$ is the joint prior distribution of shear biases and hyper-parameters, and $\pi(\hat{p}_{\hat{\epsilon}})$ is the marginal likelihood, i.e. the integral of Eq. (13) over m , c , and θ . The final posterior distribution of shear biases after marginalising over the unknown hyper-parameters is

$$\pi(m, c|\hat{p}_{\hat{\epsilon}}) = \frac{1}{\pi(\hat{p}_{\hat{\epsilon}})} \int \pi(\hat{p}_{\hat{\epsilon}}|m, c, \theta) \pi(m, c, \theta) d\theta. \quad (15)$$

The problem is now equivalent to constraining m and c statistically from an observed empirical distribution given a forward model for the true ellipticity distribution.

4 ANALYSIS

We adopted a relatively flexible model for the 1D-ellipticity distribution that broadly reproduces what is observed in real data,

$$p_\epsilon(\epsilon|\sigma, \beta, \kappa) \propto \exp \left[- \left(\frac{|\epsilon|}{\sigma} \right)^\beta \right] \left[1 - \left(\frac{|\epsilon|}{\epsilon_{\max}} \right)^\kappa \right]. \quad (16)$$

³ The relation between the empirical distribution and the standard histogram count is given by the number of samples multiplied by the bin width, such that the empirical distribution integrates to one.

The distribution includes a bell-like function with associated dispersion (σ) and exponential decay (β), and a tapering function with a decay coefficient (κ). The tapering ensures that the distribution is zero at a fixed $\epsilon_{\max} = 0.99$, which should coincide with the upper bound of the actual measurements (see, e.g., [Euclid Collaboration: Congedo et al. 2024](#)). The vector of hyper-parameters that we wish to marginalise over in the estimation of bias parameters is then $\theta = \{\sigma, \beta, \kappa\}$.

In order to ease the interpretation, we chose some representative, large values for shear biases, $m_{\text{true}} = 0.05$ and $c_{\text{true}} = -0.01$, and hyper-parameters, $\sigma_{\text{true}} = 0.3$, $\beta_{\text{true}} = 0.75$, and $\kappa_{\text{true}} = 4.0$ as ground truth. We simulated 10^7 ellipticities from the distribution of observed samples [see Eq. (4)], initially in the absence of noise, and calculated their empirical distribution, \hat{p}_ϵ , in 1000 bins, as shown in Fig. 1. We sampled the posterior of Eq. (14) with the likelihood of Eq. (13) and a wide uniform prior for biases and hyper-parameters: $m \in (-0.1, 0.1)$, $c \in (-0.1, 0.1)$, $\sigma \in (0.1, 0.6)$, $\beta \in (0.1, 2)$, and $\kappa \in (0.5, 6)$. We used the affine-invariant version of the LENS MC core sampler ([Euclid Collaboration: Congedo et al. 2024](#)) and ran 32 parallel chains of 10,000 samples after a short burn-in phase. Figure 2 shows the resulting chains with recovered mean values all within one standard deviation from the ground truth. Also, there is mild correlation between σ and β , and between β and κ , and the anti-correlation between m and κ , which can be explained in terms of those parameters being all proxies for the dispersion of the distribution. However, those degeneracies do not hinder the recovery of shear biases, thanks to marginalisation. Similar conclusions can also be drawn for smaller input biases. Finally, as a sanity check, we tested the sampling with a Gaussian likelihood and a variance term given by the observed distribution, and found fully consistent results, which corroborates the fact that the Poisson distribution converges to a Gaussian very rapidly, being already practically indistinguishable for a number of samples per bin of about 10.

The reported uncertainties in all parameters reflect the width of the posterior, after a wide, flat prior was applied. All parameters are constrained within one standard deviation and $m - m_{\text{true}} = (4 \pm 6) \times 10^{-4}$ and $c - c_{\text{true}} = (-4 \pm 9) \times 10^{-5}$. However, some parameters do show some degeneracy, made gradually worse by smaller and smaller number of data points. Since the likelihood scales as $\exp(-N)$, we tested the dependence of the biases on the recovered m and c on the number of samples, N , and found that the biases quickly converge to smaller and smaller values, and $|m - m_{\text{true}}| < 2 \times 10^{-3}$ and $|c - c_{\text{true}}| < 5 \times 10^{-5}$ for $N > 10^6$. Furthermore, we tested the impact of measurement noise on the inferred parameters with a value of σ_{ϵ_n} between 0 (nominal case) and 0.3 and a step size of 0.05. We found that the reduced χ^2 increases quadratically with σ_{ϵ_n} , with only a modest increase for $\sigma_{\epsilon_n} = 0.05$, but reaching almost 3 at 0.1. However, the biases are still reasonable: $|m - m_{\text{true}}| < 3 \times 10^{-3}$ and $|c - c_{\text{true}}| < 6 \times 10^{-5}$ for $\sigma_{\epsilon_n} = 0.1$. This level of accuracy reassures us about the sensitivity of results on the knowledge of the noise term, and gives us some leeway for the application of the methodology to real data. There are various approaches to account for measurement noise in the inference. The first is to estimate it from the data itself and then correct for it in the modelling. In fact, any shear method produces an estimate of the measurement variance (see, e.g., [Euclid Collaboration: Congedo et al. 2024](#)), so the average variance over the same selection could then be used as a convolutive kernel in the modelling. Alternatively, a Gaussian kernel could still be assumed with an unknown variance hyper-parameter to marginalise over. The downside would be the increased dimensionality and a slightly greater risk of degeneracies with other hyper-parameters. A third, more conservative option might be to still allow it as a free

parameter, but apply an informative prior based on the estimation from the data.

Crucially, the potential of this methodology is that selection biases are already correctly accounted for in the observed empirical distributions, which could be defined for a broad sample of galaxies (including tomographic bins, field-of-view positions, or morphological bins). The natural products of the inference are the effective multiplicative and additive biases after measurement and selection effects, and marginalised over the hyper-parameters of the intrinsic distribution. However, the main limitation of the methodology is primarily the accurate modelling of the intrinsic distribution. With real data, the model for the intrinsic distribution is not completely known beforehand. However, the ellipticity has to satisfy specific symmetries and boundary conditions, helping to constrain the functional form of the model. Therefore, in general, the family of functional forms should be broadly known, but the specifics of the particular function that fits the data best are not. Moreover, the multiplicative and additive biases of a well-behaved shear measurement method should usually be very small, which is already the case for Stage-III and, to a greater extent, also for Stage-IV surveys. In the limit of small, percent-level biases, their effect on the ellipticity distribution is perturbative, which means that the observed distribution will not change significantly from the true distribution. Additionally, we observed that the marginalisation mitigates the degeneracy between biases and the hyper-parameters of the distribution. All of this gives us reassurance that, under specific assumptions, it should always be possible to constrain the model from the data already available. Fortunately, deep fields could be used to constrain the functional form of the intrinsic distribution as a function of bins of interest even more precisely. These deeper observations would need to have the same selection from the wide fields applied, such that selection biases are properly accounted for.

5 CONCLUSIONS

In the context of cosmic shear surveys, we proposed a novel methodology to infer both multiplicative and additive shear biases directly from the observed distribution of galaxy ellipticities. Although the estimation of additive biases is routinely applied to real data and there is a long history of measuring shear responses on data, in this paper we provided solid theoretical grounds for the initial ansatz that multiplicative biases could also be inferred empirically from empirical distributions alongside additive biases. Using complementary statistical techniques, i.e., the transformation of probability distribution functions, their moment-generating function, and their raw and central moments, we showed that multiplicative and additive biases impact not only the mean and variance of the distribution as has been commonly assumed, but all higher moments to any order. Empirical distributions of galaxy ellipticities do help in that regard because they show a peak at zero ellipticity (potentially with a cusp), a rapid decay for increasing ellipticity, and are also truncated at $|\epsilon| < 1$ (which is a requirement of ϵ -ellipticities transforming under shear, leaving the bounds unchanged). Those distributions are highly non-Gaussian and therefore contain a lot more information than Gaussian distributions do. Therefore, the information on the biases is fully encoded in the empirical distribution to any orders and is ready to be exploited.

We introduced statistical modelling of the biased distribution, the corresponding likelihood, and a Bayesian framework to infer biases and hyper-parameters of the distribution jointly. After simulating representative data with the injection of biases and noise, we found, not so surprisingly, that additive and multiplicative biases can be

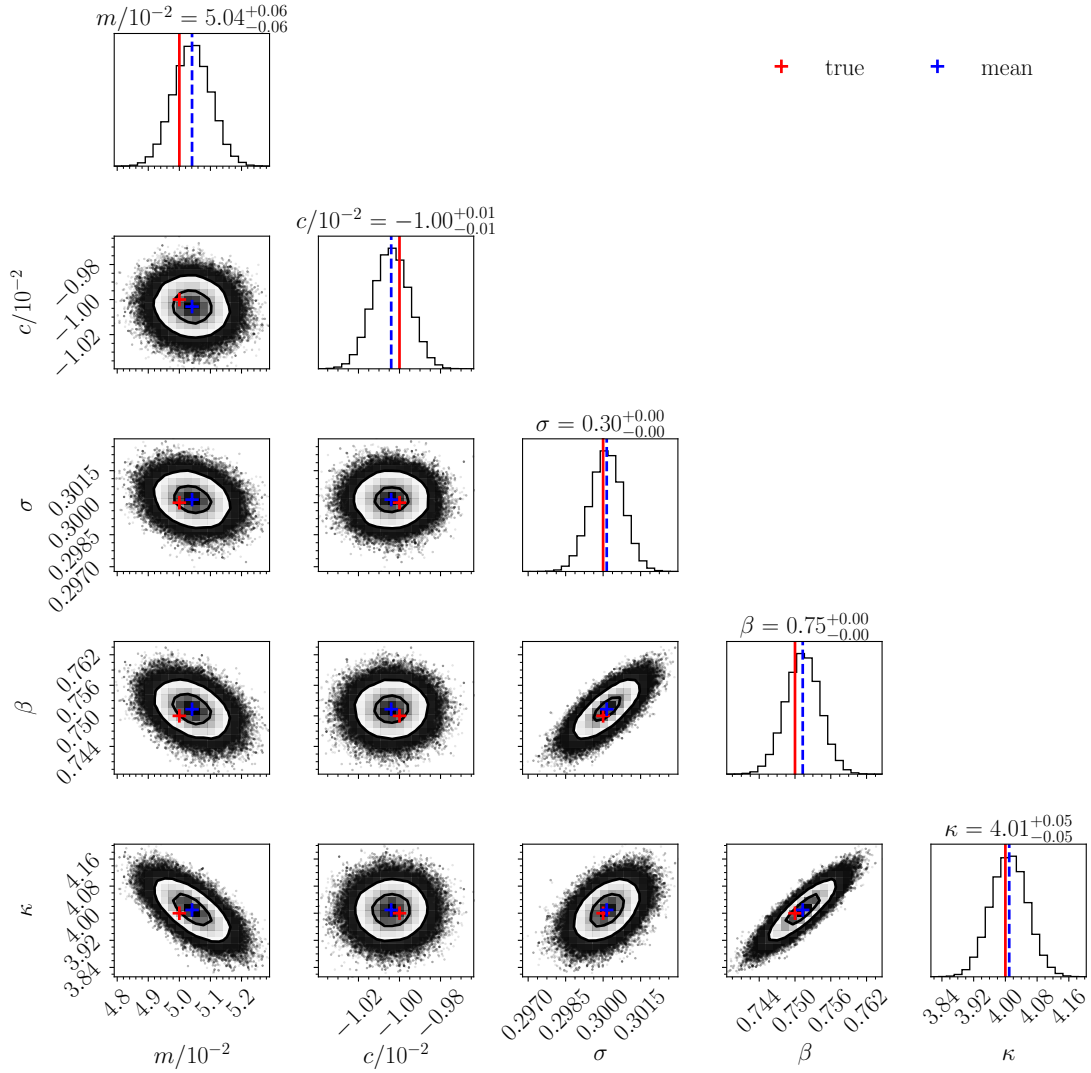


Figure 2. Joint MCMC samples of the inferred bias parameters (m and c) and distribution hyper-parameters (σ , β , and κ). The red lines/crosses represent the true values and the blue ones represent the recovered mean values marginalised over nuisance parameters. Despite the degeneracies, the marginalised m and c are constrained within one standard deviation (see the two distributions at the top left).

constrained with enough statistical power that the inferred joint distributions are not degenerate with the hyper-parameters. Meanwhile, some of the hyper-parameters are indeed correlated. However, we observed that the marginalisation significantly mitigates the sensitivity of the inferred biases on those degeneracies in the hyper-parameters. Additionally, we studied the dependence on the number of samples and Gaussian noise not captured in the modelling, which could potentially hinder the inference. We demonstrated that the biases could still be recovered with enough statistical power under reasonable conditions. Finally, we studied the potential limitations, and ways to address them on real data.

We envisage that our methodology is very general and has a wide range of applicability to weak lensing surveys. Therefore, it warrants detailed investigation on real data from Stage-IV surveys, especially *Euclid* and *Rubin* where the accuracy requirements are stringent and measurements have to be calibrated with simulations. Being agnostic of cosmology and galaxy morphology, our self-calibration of cosmic shear biases could not only aid the calibration with simulations by

providing useful empirical priors for biases, but also alleviate the reliance on large-scale, realistic simulations, which are usually one of the most difficult tasks of lensing analyses.

ACKNOWLEDGEMENTS

GC and ANT acknowledges support provided by the United Kingdom Space Agency. ANT acknowledges support provided by the Science and Technology Facilities Council. Figure 2 was made with corner (Foreman-Mackey 2016).

REFERENCES

- Antilogus P., Astier P., Doherty P., Guyonnet A., Regnault N., 2014, *J. Instrum.*, **9**, C03048
 Bernstein G. M., Armstrong R., 2014, *MNRAS*, **438**, 1880

- Bernstein G. M., Armstrong R., Krawiec C., March M. C., 2016, *MNRAS*, **459**, 4467
- Cropper M., et al., 2013, *MNRAS*, **431**, 3103
- Euclid Collaboration: Congedo G., Miller L., Taylor A. N., et al., 2024, *A&A*, **691**, A319
- Euclid Collaboration: Martinet N., et al., 2019, *A&A*, **627**, A59
- Euclid Collaboration: Mellier Y., et al., 2025, *A&A*, **697**, A1
- Fenech Conti I., Herbonnet R., Hoekstra H., Merten J., Miller L., Viola M., 2017, *MNRAS*, **467**, 1627
- Foreman-Mackey D., 2016, *J. Open Source Softw.*, **1**, 24
- Guzik J., Bernstein G., 2005, *Phys. Rev. D*, **72**, 043503
- Hall A., Taylor A., 2017, *MNRAS*, **468**, 346
- Heymans C., et al., 2006, *MNRAS*, **368**, 1323
- Hildebrandt H., et al., 2020, *A&A*, **633**, A69
- Hoekstra H., 2021, *A&A*, **656**, A135
- Hoekstra H., Viola M., Herbonnet R., 2017, *MNRAS*, **468**, 3295
- Hoekstra H., Kannawadi A., Kitching T. D., 2021, *A&A*, **646**, A124
- Huff E., Mandelbaum R., 2017, *arXiv:1702.02600*
- Huterer D., Takada M., Bernstein G., Jain B., 2006, *MNRAS*, **366**, 101
- Ivezić Ž., et al., 2019, *ApJ*, **873**, 111
- Jansen H., Tewes M., Schrabback T., et al., 2024, *A&A*, **683**, A240
- Joachimi B., et al., 2015, *Space Sci. Rev.*, **193**, 1
- Kannawadi A., et al., 2019, *A&A*, **624**, A92
- Kilbinger M., 2015, *Rep. Prog. Phys.*, **78**, 086901
- Kitching T., Deshpande A., Taylor P., 2021, *Open J. Astrophys.*, **4**, 17
- Li X., et al., 2022, *PASJ*, **74**, 421
- Li S.-S., et al., 2023a, *A&A*, **670**, A100
- Li S.-S., et al., 2023b, *A&A*, **679**, A133
- MacCrann N., Becker M. R., McCullough J., et al., 2022, *MNRAS*, **509**, 3371
- Mandelbaum R., et al., 2018, *MNRAS*, **481**, 3170
- Massey R., et al., 2013, *MNRAS*, **429**, 661
- Melchior P., Viola M., 2012, *MNRAS*, **424**, 2757
- Miller L., et al., 2013, *MNRAS*, **429**, 2858
- Paulin-Henriksson S., Amara A., Voigt L., Refregier A., Bridle S. L., 2008, *A&A*, **484**, 67
- Pujol A., Kilbinger M., Sureau F., Bobin J., 2019, *A&A*, **621**, A2
- Refregier A., Kacprzak T., Amara A., Bridle S., Rowe B., 2012, *MNRAS*, **425**, 1951
- Rhodes J., Leauthaud A., Stoughton C., Massey R., Dawson K., Kolbe W., Roe N., 2010, *PASP*, **122**, 439
- Schneider P., 2005, *arXiv:astro-ph/0509252*
- Seitz C., Schneider P., 1997, *A&A*, **318**, 687
- Sheldon E. S., 2014, *MNRAS*, **444**, L25
- Sheldon E. S., Huff E. M., 2017, *ApJ*, **841**, 24
- Sheldon E. S., Becker M. R., MacCrann N., Jarvis M., 2020, *ApJ*, **902**, 138
- Sheldon E. S., Becker M. R., Jarvis M., Armstrong R., LSST Dark Energy Science Collaboration 2023, *Open J. Astrophys.*, **6**, 17
- Spergel D., et al., 2015, *arXiv:1503.03757*
- van Uitert E., Schneider P., 2016, *A&A*, **595**, A93

This paper has been typeset from a $\text{\TeX}/\text{\LaTeX}$ file prepared by the author.